Heliyon 10 (2024) e39717

Contents lists available at ScienceDirect

Heliyon

journal homepage: www.cell.com/heliyon

Research article

Eco-friendly *Chlorella vulgaris* extracts for corrosion protection of steel in acidic environments

Edgar Almanza [a], Lizeth Del Carmen Gutierrez Pua [b,*], Yaneth Pineda [c], Wilson Rozo [d], Mauricio Marquez [a], Ana Fonseca [b,**]

[a] Department of Mechanical Engineering, Universidad Autónoma del Caribe, Colombia
[b] Department of Mechanical Engineering, Universidad del Norte, Barranquilla, Colombia
[c] Department of Metalurgical Engineering, Universidad Pedagógica y Tecnológica de Colombia, Colombia
[d] Department of Chemistry, Universidad Pedagógica y Tecnológica de Colombia, Colombia

ARTICLE INFO

Keywords:
Corrosion inhibition
Chlorella vulgaris
Microalgae inhibitors
Green inhibitors
Steel pipeline systems

ABSTRACT

This study evaluates the potential of Chlorella vulgaris sp. extracts as eco-friendly corrosion inhibitors for API 5L 42 Steel in a 1M HCl acidic environment, offering sustainable alternatives for industrial applications. Two corrosion inhibitors were obtained through solvent extraction methods: M1 (methanol) and M2 (methanol/chloroform). The extracts were characterized using infrared spectroscopy, the analysis revealed hydroxyl, methyl and vinyl groups as the most representative. The effect of corrosion inhibition was study by electrochemical impedance spectroscopy (EIS) and potentiodynamic polarization. The results show significant reductions in corrosion current density and increases in charge transfer resistance, with M2 achieving the highest protection efficiency of 91.20 % and a charge transfer resistance of 501.80 Ω at a 120 ppm concentration, while M1 reached 88.22 % efficiency with a charge transfer resistance of 102.30 Ω. Uv–Vis measurements were performed to determine the electronic transitions of the metal-inhibitor system for each of the extracts. ANOVA highlighted the significant influence of biomass concentration on corrosion resistance. The adsorption of M1 and M2 extracts on the carbon steel surface obeyed the Langmuir isotherm and Gibbs free energy calculations indicated a physisorption mechanism for both extracts. Surface morphology analysis by Scanning electron microscope (SEM) revealed less pitting and reduced surface roughness as inhibitor concentration increased. These findings underscore the potential of Chlorella vulgaris extracts, particularly M2 at 120 ppm, as effective and sustainable corrosion inhibitors for steel in acidic environments.

1. Introduction

Corrosion in pipelines and steel structures represents a critical and ongoing issue, resulting in material degradation and elevated maintenance [1–5] This problem is notably pronounced in underground metal conduits, which are susceptible to stress-induced

* Corresponding author.
** Corresponding author.
E-mail addresses: Edgarg.almanza@gmail.com (E. Almanza), gutierrezdl@uninorte.edu.co (L. Del Carmen Gutierrez Pua), Yaneth.pineda@uptc.edu.co (Y. Pineda), Wilson.rozo@uptc.edu.co (W. Rozo), Mauricio.marquez45@uac.edu.co (M. Marquez), fonsecama@uninorte.edu.co (A. Fonseca).

https://doi.org/10.1016/j.heliyon.2024.e39717
Received 30 July 2024; Received in revised form 21 October 2024; Accepted 22 October 2024
Available online 23 October 2024

cracking and hydrogen-assisted embrittlement, leading to diminished structural integrity and increased failure susceptibility [5–7]. The global economic impact of corrosion is substantial, with costs estimated to reach up to $2.5 trillion [8]. Conventional anti-corrosion strategies, including coatings and galvanization, often exhibit limited efficacy, thereby necessitating the development of more advanced and environmentally benign inhibitors derived from natural sources [9–12].

Green inhibitors are those extracted from plants or natural structures that provide a protective molecular layer at the metal-solution interface through physisorption processes via the electrostatic interaction of the inhibitor molecule with the metallic surface [12,13]. These inhibitors typically contain elements such as nitrogen, sulfur, oxygen, phosphorus, and feature multiple bonds or aromatic rings. In this regard, compounds like plant extracts, chitosan, and cellulose have structures or functional groups that can act as green corrosion inhibitors. Additionally, amino acids, the building blocks of proteins, have emerged as excellent candidates for green inhibitors due to their high purity and availability, low cost, and structural characteristics that enhance absorption and inhibition performance [13–15].

The use of green inhibitors has been reported in several applications, including plant extracts [16–28], henna leaves [29], European fan palm (*Chamaerops humilis*), parsley, lettuce, and radish [30], curcumin, and cassia bark [31], vegetables oils [12], black pepperpotato [32], saffron [33], bitter orange leaf [34], Citrus Peel Waste [35], licorice [36], marine sponges [37], biopolymers like Polyaniline [35], pharmaceutical drugs (levofloxacin, moxifloxacin, metolazone, and nifedipine) [38], as well as marine and terrestrial algae such as *Caulerpa racemose* [39]*, Hydroclathrus clathratus* [40] *Prasiola crispa* [41].

Microalgae have attracted attention due to their diverse composition and versatile applications. These photosynthetic microorganisms can be used to produce various metabolites, such as lipids, proteins, and pigments [42]. They have a high content of vitamins, fatty acids, essential amino acids, and polysaccharides. Over recent years, they have been extensively researched across various fields including the food industry, medical and pharmaceutical applications, chemical industries, biofuels, renewable energy sources, and water treatment, among others, demonstrating promising outcomes [43–46].

Several studies have highlighted microalgae as effective green corrosion inhibitors for steels, demonstrating impressive inhibition efficiencies. *Spirulina máxima* [47] and *Chlorella sorokiniana* [48] showed inhibition efficiencies of 96.4 % and 94.6 %, respectively, forming protective films through biomolecule adsorption such as proteins. *Scenedesmus* sp. achieved up to 95.1 % inhibition efficiency using fatty acids like C18:3, C18:2, and C16:0, stablishing a robust metal-inhibitor framework. *Spirulina platensis* effectively inhibited steel corrosion by 66 % under acidic conditions, following the Temkin isotherm with efficiency increasing with concentration [49,50]. *Arthrospira platensis* demonstrated 66 % efficacy in HCl media due to phytochemical compounds like saponins and steroids, confirmed by FTIR and SEM analyses following Langmuir adsorption isotherm principles [50]. Fatty acids from *Scenedesmus* sp. effectively inhibited mild steel corrosion in 1 M HCl, achieving 95.1 % inhibition at 36 ppm concentration, supported by electrochemical analysis. Surface studies revealed altered morphology and reduced hydrogen evolution, highlighting their strong adsorption capacity [51]. Additionally, microalgae extract from *Chlorococcum* sp. inhibited mild steel corrosion by 96 % in acidic environments, forming a stable protective layer rich in levoglucosenone and hexadecanoic acid. Electrochemical tests confirmed enhanced surface resistance and increased energy barriers against corrosion reactions [52].

Chlorella vulgaris. distinguishes itself from other Microalgae such as *Spirulina maxima, Scenedesmus* sp., and *Chlorococcum* sp. due to its superior biochemical composition and cultivation advantages. This unicellular green algae is particularly notable for its high nutritional content: it contains approximately 61.6 % protein, 20–32 % lipids, and 13.7 % carbohydrates [53–55] Additionally, *Chlorella vulgaris* is rich in essential nutrients, including various vitamins (such as folic acid, vitamin C, vitamin B complex, and vitamin D), minerals (like iron, potassium, and magnesium), and a range of phytochemicals (such as lutein, β-carotene, and chlorophyll) [54]. This diverse nutrient profile may enhance its efficacy as a corrosion inhibitor compared to other microalgae. For instance, *Spirulina maxima* have 50–70 % protein, 6–13 % lipids, and 15–25 % carbohydrates [56]. *Scenedesmus* sp. is also protein-rich, with 8–56 % protein, 12–14 % lipids, and 10–18 % carbohydrates [57]. *Chlorococcum* sp. shows a maximal carbohydrate content of 63.7 % and a protein content of 27.3 % [58]. Lipids are particularly effective in forming protective films on metal surfaces. These hydrophobic films act as a physical barrier, reducing the corrosion rate by preventing contact between the metal and corrosive agents like water and acids [59,60] The high lipid content in *Chlorella vulgaris* may significantly enhance its ability to create such protective layers, offering superior corrosion protection. Additionally, proteins play a crucial role as corrosion inhibitors due to their functional groups (such as amino and carboxyl groups) that can interact with metal surfaces [61–63] The combination of a high lipid profile and substantial protein content in *Chlorella* makes it an especially attractive candidate for use as a green corrosion inhibitor.

In terms of cultivation, *Chlorella vulgaris* is particularly noteworthy for its ability to thrive in a broad range of temperatures, making it suitable for successful cultivation in several natural environments and a strong candidate for high-rate outdoor production systems [64,65]. Additionally, it can grow in a pH range of 4–10, with optimal biomass production occurring between pH 9 and 10 [46]. This adaptability further distinguishes *Chlorella vulgaris* as a versatile and robust species for industrial applications. Finally, *Chlorella vulgaris* is among the most extensively cultivated microalgae worldwide, with significant production occurring in countries like the United States, Germany, and Japan [66]. The global market for *Chlorella* was valued at approximately USD 275.21 million in 2021 and is expected to grow to USD 506.99 million by 2030. This represents a compound annual growth rate (CAGR) of 6.3 % over the forecast period, rising from USD 292.55 million in 2022 [67].

Building on the established effectiveness of microalgae as eco-friendly corrosion inhibitors and the distinctive biochemical profile of *Chlorella vulgaris*, this study investigates the efficacy of this microalga as a corrosion inhibitor. The research involves the synthesis of two distinct extracts from *Chlorella vulgaris* and their application to API 5L 42 Steel in a 1M HCl acidic environment. The study evaluates the potential of these extracts to serve as superior inhibitors by examining the effects of different concentrations on corrosion resistance. Evaluation methods include electrochemical and gravimetric tests, along with chemical and morphological characterization. Additionally, statistical validation was employed to ensure the reliability and accuracy of the results.

2. Materials and methods

2.1. Materials

The study utilized a carbon steel with the following composition: Mn (0.51 %), Si (0.17 %), C (0.19 %), Cr (0.14 %), Ni (0.09 %), and trace elements of P, S, Cu, Mo, and V, with the remaining constituent being Fe. Specimens measuring 2 cm × 1.5 cm x 0.5 cm were prepared for gravimetric tests, while cylindrical specimens with an exposed area of 1.2 cm^2 were employed for electrochemical assays. Prior to testing, the steel surfaces were abraded using SiC abrasive paper ranging from 80 to 2000 grit. After abrasion, specimens were thoroughly rinsed with distilled water, cleaned with acetone to eliminate any surface residues, and dried using compressed air.

Analytical grade methanol and chloroform solvents were used in the extraction process of Chlorella vulgaris biomass. Analytical grade hydrochloric acid at 37 % concentration in a 1 M solution served as the electrolyte for corrosion tests. *Chlorella vulgaris* was sourced from Ciénaga de Mallorquin, Barranquilla, Atlántico, Colombia.

2.2. Preparation of Chlorella vulgaris-based corrosion inhibitors

2.2.1. Isolation and growth condition of microalgal strain

The step-by-step process for preparing the extracts is illustrated in Figs. 1 and 2. *Chlorella vulgaris* was sourced from Ciénaga de Mallorquin, Barranquilla, Atlántico, Colombia. A pre-culture was prepared using 247 mL of distilled water and 3 mL of microalgae under 24-h photoperiods. 0.5 g of Soybean Flour (Glycine max) were added to promote biomass growth [62,63], and the pre-culture was maintained under constant agitation (Fig. 2a*)*. After one week, the pre-culture was centrifuged to obtain the initial biomass, which was used to scale up the culture in a 5 L photobioreactor (Fig. 2b*)*. The culture was maintained under 24-h photoperiods, constant air supply, and fed every 2 days with 5 g of Soybean flour. On day 14, the culture was centrifuged to harvest the biomass used to obtain the corrosion inhibitors (Fig. 2c*)*.

2.2.2. Extraction protocol for Chlorella vulgaris inhibitors

The inhibitors were prepared using extracts from *Chlorella vulgaris* biomass, employing both a polar protic solvent (methanol, CH_3OH) and an aprotic solvent (chloroform, $CHCl_3$) as outlined in Fig. 1. Two distinct extraction methods were utilized: for Extract 1 (M1), the biomass was mixed with methanol, stirred at room temperature, filtered, and dried using a rotary evaporator to obtain a methanol-based extract (Fig. 2d*)*. For Extract 2 (M2), the biomass was treated with a combination of chloroform and methanol, followed by sonication, centrifugation, and liquid-liquid separation. The organic phase from M2 was dried, and both final extracts were dissolved in methanol for use as corrosion inhibitors.

2.3. Fourier Transform Infrared Spectroscopy: Characterization of extracts

Fourier Transform Infrared Spectroscopy (FTIR) spectra of *Chlorella vulgaris* extracts were acquired using a Prestige 21 Shimadzu FTIR instrument. The spectra were recorded over the frequency range of 4500 to 600 cm^{-1} to investigate the functional groups present in extracts M1 and M2.

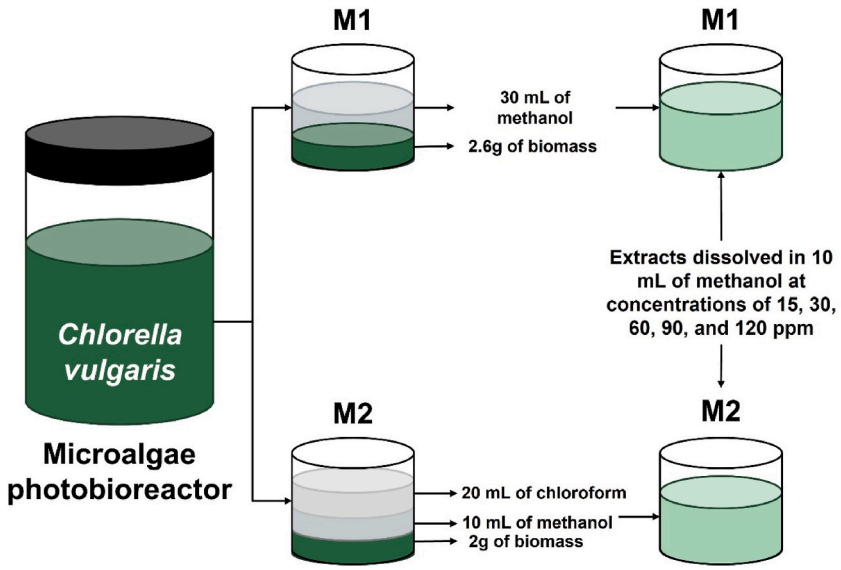

Fig. 1. Extraction of Chlorella vulgaris sp. biomass for corrosion inhibitors.

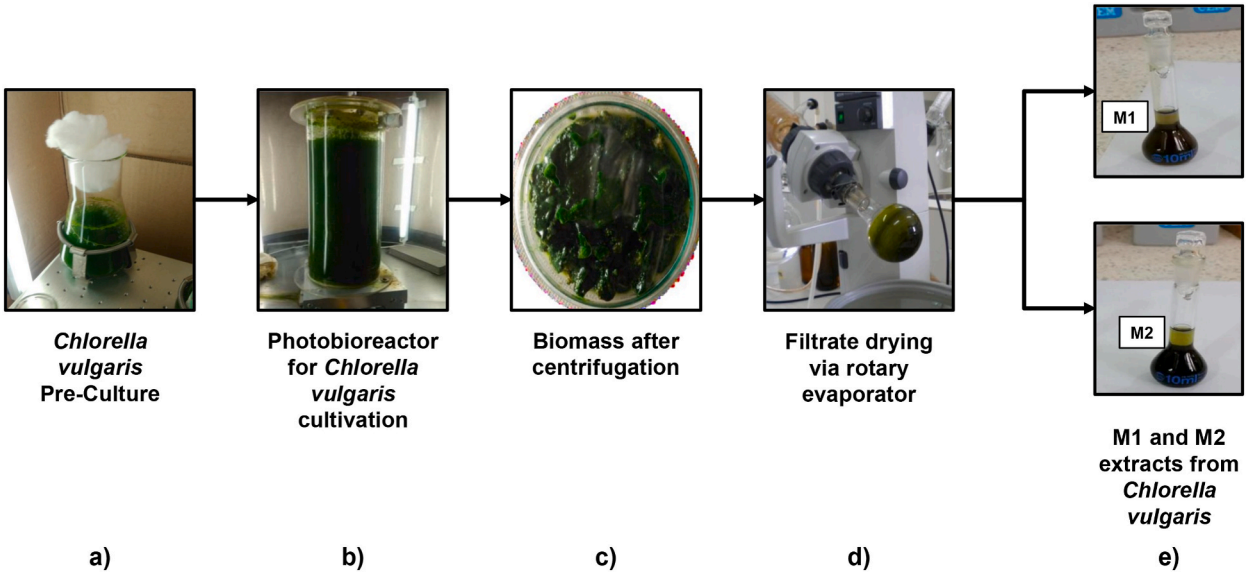

Fig. 2. Step-by-step extraction procedure for green corrosion inhibitors: a) Pre-culture of Chlorella vulgaris, b) Photobioreactor for cultivation, c) Biomass centrifugation, d) Filtrate drying using a rotary evaporator, and e) Final M1 and M2 extracts from Chlorella vulgaris.

2.4. Electrochemical measurements

Corrosion behavior measurements were conducted in a conventional three-electrode cell setup. Ag/AgCl served as the reference electrode, platinum as the auxiliary electrode, and steel specimens as the working electrode with an exposed area of 1.2 cm^2, immersed in a 1 M HCl solution as the electrolyte. Electrochemical impedance spectroscopy (EIS) curves were obtained using a potentiostat/galvanostat (Gamry 750). EIS was performed at open circuit potential (OCP) with frequencies ranging from 100 kHz to 0.01 Hz, applying a perturbation amplitude of 5 mV. Corrosion parameters, including corrosion potential (E_{corr}) and corrosion current density (i_{corr}), were determined using Tafel extrapolation method over an overpotential range of −0.25 to 0.25 V relative to OCP. Electrochemical measurements were performed in triplicate at room temperature.

To assess the efficiency of the inhibitors via impedance electrochemical and potentiodynamic analysis, equations (1) and (2) were employed [51,68,69]:

$$\%\eta = \frac{i_{corr\,without-inh} - i_{corr\,inh}}{i_{corr\,without-inh}} * 100\% \quad (1)$$

Where $i_{corr\,without-inh}$ y $i_{corr\,inh}$ correspond to the corrosion current densities in the absence and presence of the inhibitor, respectively.

$$\%\eta = \frac{R_{ct\,with-inh} - R_{ct\,without-inh}}{R_{ct\,with-inh}} * 100\% \quad (2)$$

Where $R_{ct\,with-inh}$ and $R_{ct\,without-inh}$ correspond to the resistance to charge transfer in the presence and absence of the inhibitor, respectively.

2.5. Gravimetric tests

For the gravimetric evaluation, specimens were immersed in 70 mL of 1 M HCl and categorized based on the concentration of the extract used: SS, SS-15, SS-30, SS-60, and SS-120. The specimens were weighed both before and after exposure. Each sample was submerged in the HCl solution for 3 h at room temperature. The mass loss of the specimens, the corrosion rate (CR), and the efficiency of the inhibitors (%η) were determined following ASTM G31 [70] standards. The corrosion rate (CR) and inhibitor efficiency (%η) were calculated using Equations (3) and (4), respectively. The specific equations used to estimate these variables are referenced in Refs. [51, 68,69]:

$$CR = \frac{\Delta W \times 8.76 \times 10^4}{(A \bullet t \bullet D)} \quad (3)$$

$$\%\eta = \frac{(CR_{without-inh}) - (CR_{inh})}{CR_{without-inh}}.100\% \quad (4)$$

Where CR is the corrosion rate of the steel, ΔW represents the mass loss of the specimen in grams, A corresponds to the exposed area during the test (cm^2), t is the exposure time in hours, D is the density of the material, and 8.76×10^4 is the conversion factor to express the corrosion rate in millimeters per year (Equation (2)). For the efficiency (Equation (4)), $CR_{without-inh}$ y CR_{inh} are the corrosion rates of the specimens without and with inhibitor, respectively, measured in triplicate.

2.6. Adsorption isotherms

The application of adsorption isotherms facilitates the calculation of surface coverage degrees (θ) using Equation (5) for various concentrations in 1.0 M HCl at 298 K, based on the corrosion current density values derived from potentiodynamic polarization measurements. Three adsorption models were evaluated: Langmuir, Temkin, and Frumkin.

$$\theta = \frac{icorr^0 - icorr^{inh}}{icorr^0} \tag{5}$$

2.7. UV–visible spectroscopy

A Shimadzu UV2600 spectrophotometer was used to perform UV–visible spectroscopy over a wavelength range of 200–400 nm. This analysis aimed to investigate the formation of inhibitor complexes from M1 and M2 in 1 M HCl following the immersion process of carbon steel.

2.8. Surface analysis

A qualitative analysis of the steel surface was conducted before and after immersion testing in 1 M HCl for 3 h. A scanning electron microscope (Carl Zeiss EVO MA10) was used to observe the inhibitory effect of each concentration of the studied species.

2.9. Stadistical analysis

Based on the results obtained from Electrochemical Impedance Spectroscopy (EIS), a one-way analysis of variance (ANOVA) was performed using the charge transfer resistance (R_{ct}) obtained from fitting the equivalent circuit (Fig. 2e). This analysis was conducted to determine if there is a significant difference in the corrosion resistance of the steel after treatment with the inhibitors. For each concentration of the extracts M1 and M2, a sample size of $n = 3$ was considered. Fisher's least significant difference (LSD) test was then applied to identify which evaluated concentration provides the best performance (highest resistivity). Both tests were conducted at a 95 % confidence level ($\alpha = 0.05$).

Additionally, for the gravimetric analysis, ANOVA was conducted to determine the influence of biomass concentration in the extract on the corrosion rate mitigated by the inhibitor, again using a sample size of $n = 3$ for each concentration of M1 and M2. The statistical analyses were conducted using RStudio, Version 4.2.2.

3. Results

3.1. Extraction and preparation of Chlorella-based inhibitors

The extracts were prepared as follows.

- **Extract 1 (M1):** 2.6 g of *Chlorella vulgaris* biomass were mixed with 30 mL of methanol. The solution was continuously stirred for 24 h at room temperature (25 °C). Subsequently, the mixture was filtered, and the remaining biomass on the filter was rinsed with 10 mL of methanol. Both filtrates were combined and dried using a rotary evaporator (Fig. 2d). Finally, the remaining extract was dissolved in 2 mL of methanol and used as an inhibitor.
- **Extract 2 (M2):** Two grams of *Chlorella vulgaris* biomass were mixed with 20 mL of chloroform and 10 mL of methanol. The solution was sonicated for 10 min and stirred for 12 h at 25 °C. The mixture was then centrifuged at 5000 rpm for 15 min to obtain the supernatant. The same volumetric ratio of chloroform and methanol was added to the sediment, followed by a second centrifugation under the same conditions. The supernatants were combined, and 20 mL of chloroform and 20 mL of distilled water were subsequently added. After phase separation, the lower organic phase was recovered and dried using a rotary evaporator. The remaining residue was dissolved in 2 mL of methanol and used as the inhibitor (Fig. 2).

The dosages used in this study involved dissolving the extracts in 10 mL of methanol at concentrations of 15, 30, 60, 90, and 120 ppm, as previously reported in the literature [71–73].

3.2. Fourier transform infrared spectroscopy

Fig. 3 displays the FTIR spectra for M1 and M2 and Table 1 shows the spectral bands with their corresponding biomolecular functional group and origin. In the spectrum of M1, a broad hydroxyl group stretching band is observed between 3600 and 2600 cm^{-1},

with overlapping peaks below 3000 cm^{-1} (Fig. 3a). At 1580 cm^{-1}, an asymmetric absorption of the conjugated vinyl group (-C=C-) is detected, while the methylene bending vibration appears at 1408 cm^{-1}. Additionally, signals corresponding to the C-O bond are observed at 1074 and 1043 cm^{-1}. For M2, a broad stretching band of the hydroxyl group (-OH) is present between 3600 and 2600 cm^{-1} (Fig. 3b). The asymmetric and symmetric stretching of methylene groups (-CH_2-) is seen at 2924 and 2853 cm^{-1}, respectively. A carbonyl group (-CO-) is indicated by a peak at 1705 cm^{-1}. The asymmetric vinyl group (-C=C-) signal is found at 1580 cm^{-1}, and the methylene bending vibration appears at 1408 cm^{-1}. Finally, the C-O bond is observed at 1080 cm^{-1}.

These signals suggest that the extracts are composed of a mixture of molecules containing both oxygenated groups and hydrocarbon chains. Specifically, the presence of hydroxyl groups (OH), carboxyl groups (COOH), and methylene (-CH_2-) groups indicates the involvement of polysaccharides, esters, and carboxylic acids, consistent with biomolecular structures such as lipids and proteins [74,75,77]. The absorption peaks in the 1200–1000 cm^{-1} range are also associated with carbohydrates, likely indicating the presence of polysaccharides [75,76]. These findings suggest a complex molecular composition in the extracts, providing further evidence of the functional groups involved in the corrosion inhibition mechanism.

3.3. Electrochemical evaluation

3.3.1. Electrochemical impedance spectroscopy

EIS was used to assess charge transfer processes at the metal-electrolyte interface under varying concentrations of inhibitors M1 and M2. The Nyquist plots in Fig. 4a and c, reveal a single capacitive loop, whose diameter increases with each inhibitor concentration, demonstrating the protective capability of green species against steel corrosion reactions ($Fe = Fe^{+2} + 2e^{-}$), compared to the control sample of steel in 1M HCl without inhibitor.

Similarly, in the Bode plots (Fig. 4b and d) higher impedance modules are observed at high frequencies for all concentrations of inhibitors M1 and M2 compared to the control sample of steel in 1M HCl without inhibitor, confirming the inhibitory capacity of the microalgae *Chlorella Vulgaris* sp. on steel. The maximum impedance module value at low frequencies indicates superior protective performance for both M1 and M2 [78]. The phase angle (Fig. 4b and d) also increases with increasing concentration of each inhibitor; a larger phase angle implies more capacitive behavior and a more passive surface. This confirms the adsorption of inhibitors on the metal surface, resulting in slower charge transfer processes and hence greater corrosion resistance [79–81].

For fitting the electrochemical impedance data, the Gamry Echem Analyst software was employed, utilizing the equivalent electrical circuit depicted in Fig. 4e. In this circuit, Rs denotes the solution resistance, CPE represents a constant phase element employed to account for surface roughness effects, and Rct is the charge transfer resistance at the steel-electrolyte interface. The impedance of a CPE (Z_{CPE}) is given by equation (6):

$$Z_{CPE} = Q^{-1}(j\omega)^{-n} \tag{6}$$

where Q is the CPE factor, ω\omegaω is the angular frequency ($\omega = 2\pi f$), n is the deviation index, and j is the imaginary unit. The value of n is critical as it helps identify the components defining the equivalent circuit, with n values of $1, 0.5, 0, -0.5$ or -1 corresponding to capacitance, resistance, or inductance, respectively [82]. The CPE magnitude, R_{ct}, and the phase shift (n) were used to calculate the double-layer capacitance (C_{dl}) using equation (7):

$$C_{dl} = Q^{-1/n} R_{ct}^{1-n/n} \tag{7}$$

Table 2 presents the electrochemical parameters derived from the fitting of the EIS data. The results indicate that R_{ct} increases with

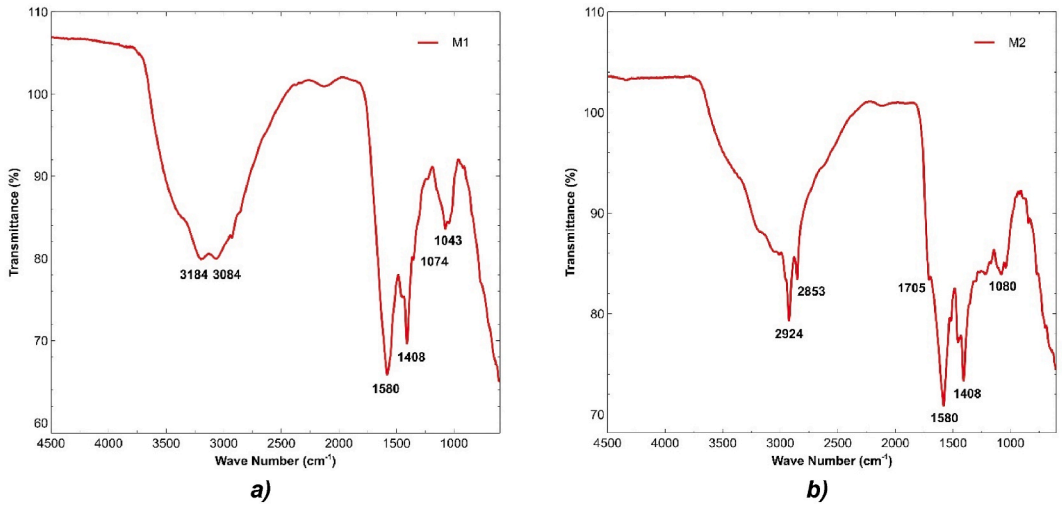

Fig. 3. FTIR spectra for a) M1 and b) M2 extracts.

Table 1
FTIR spectral bands and their corresponding biomolecular functional group.

Wave range (cm^{-1})	M1 (cm^{-1})	M2 (cm^{-1})	Functional Group	Biomolecular origin	Ref.
3500–3100	3184	–	O-H stretching with hydrogen bonds	Polysaccharides	[74]
3000–2800	3084	2924	Aliphatic	Mainly lipid	[74–76].
		2853	C-H Stretch		
1750–1700	–	1705	Ester, Ketone, and Carboxylic Acid (C=O) Stretch	Lipids, Chlorophyll, Carotenoid Pigments	[74].
1585–1481	1580	1580	Amide C-N Stretch and N-H bend	Protein (Amide II)	[77,75].
1440–1395	1408	1408	Asymmetric flexion of CH3	Protein	[75]
~1200–980	1074	1080	C-O-C Stretch	Polysaccharides	[75,76]
	1043				

the addition of M1 and M2, suggesting an enhancement in the resistance to charge transfer at the steel-electrolyte interface. This increase implies the formation of a protective layer on the steel surface. Additionally, the observed decrease in C_{dl} with rising concentrations of M1 and M2 suggests either a reduction in the thickness of the double layer, a change in the local dielectric constant, or an increased coverage of the steel surface by the inhibitors [83]. Thus, it can be inferred that the *Chlorella vulgaris* extract affects the double layer structure by displacing adsorbed water molecules and other ions, thereby reducing the steel dissolution rate. This interaction results in increased corrosion resistance, likely due to the formation of a protective layer on the steel surface. The rise in R_{ct} following the addition of M1 and M2 is indicative of enhanced resistance to corrosion, reflecting both the dissolution and repassivation processes at the interface as well as the electronic conductivity of the protective film. Consequently, the efficiencies achieved are 79.01 % for M1 and 95.72 % for M2.

Khanra, reported an inhibition efficiency of 88.2 % for fatty acid molecules from the microalga *Scenedesmus* sp. at a concentration of 36 ppm [51]. Rodrigues and Do Valle, observed an inhibition efficiency of 96.4 % for *Spirulina maxima* at 800 ppm [47]. Oliveira, documented a 95.5 % inhibition efficiency for *Chlorella sorokiniana* at 800 ppm using electrochemical impedance [84]. In comparison, the extracts of *Chlorella vulgaris* (M1 and M2) exhibit exceptional performance, achieving similar efficiencies at a much lower concentration of 120 ppm without requiring complex molecular separation processes.

An analysis of variance (ANOVA) was performed to assess the impact of *Chlorella vulgaris* biomass concentration on charge transfer resistance in the steel-electrolyte system for both M1 and M2 inhibitors. Fisher's least significant difference (LSD) test was then used to compare mean resistance levels across different inhibitor concentrations.

For M1 inhibitors, the biomass concentration had a statistically significant effect on charge transfer resistance (p-value: 1.0298E-06) at a 95 % confidence level. LSD analysis revealed two distinct resistance levels: concentrations ranging from 15 ppm to 90 ppm did not exhibit statistically significant differences, whereas at 120 ppm, the steel demonstrated significantly higher resistance compared to the inhibitor-free control, indicating enhanced corrosion protection.

For M2 inhibitors, biomass concentration also significantly affected steel resistivity (p-value: 8.6391E-16). LSD analysis identified five distinct resistance levels: all concentrations except 15 ppm and 30 ppm showed statistically significant differences as the concentration of the extract increased. The 120 ppm concentration provided the highest level of corrosion resistance for steel.

3.3.2. Potentiodynamic curves

Fig. 5 displays the potentiodynamic polarization curves, illustrating the effect of M1 (Fig. 5a) and M2 (Fig. 5b) on the electrochemical behavior of steel exposed to 1M HCl. Table 3 presents the results of Tafel slope extrapolation fitting, where β_a and β_c represent the anodic and cathodic slopes respectively, i_{corr} denotes corrosion current density, E_{corr} is the corrosion potential, and η indicates the inhibition efficiency of M1 and M2 inhibitors.

The fitting results indicate surface protection of the steel by reducing corrosion current density for all concentrations compared to steel exposed to 1M HCl solution [85,86]. Additionally, a shift in corrosion potential towards more positive values, exceeding ± 85 mV relative to inhibitor-free steel, suggests that inhibitors act by controlling the anodic dissolution reaction ($Fe = Fe^{+2} + 2e^{-}$) [87]. The decrease in corrosion current density across evaluated concentrations compared to steel exposed to 1M HCl solution also suggests inhibitor adsorption on the steel surface, gradually improving efficiency. Furthermore, a significant decrease in βa was observed for all concentrations of M1 and M2 compared to inhibitor-free steel, indicating a slower electrochemical reaction and thus better corrosion resistance. Consequently, maximum efficiencies of 97.14 % and 99.09 % were achieved for M1 and M2 respectively at a concentration of 120 ppm.

Authors such as Rodrigues and Do Valle reported an inhibition efficiency of 93.9 % for *Spirulina maxima* at a concentration of 800 ppm [47], while Oliveira reported an efficiency of 94.8 % for *Chlorella sorokiniana* at 800 ppm using potentiodynamic polarization [84]. These findings underscore the superior performance of *Chlorella vulgaris* extracts M1 and M2, which demonstrate higher inhibition efficiencies at a significantly lower concentration of 120 ppm.

3.4. Gravimetric analysis

Fig. 6 shows the efficiency of the inhibitors and the steel corrosion rate for the different extracts used. It is observed that for both M1 (Fig. 6a) and M2 (Fig. 6b), he corrosion rate decreases progressively with increasing concentrations of each inhibitor, leading to a corresponding increase in protection efficiency. The results indicate that both inhibitors achieve efficiencies greater than 80 % across all tested concentrations, with maximum protection efficiencies of 88.22 % for M1 and 91.20 % for M2 at a concentration of 120 ppm.

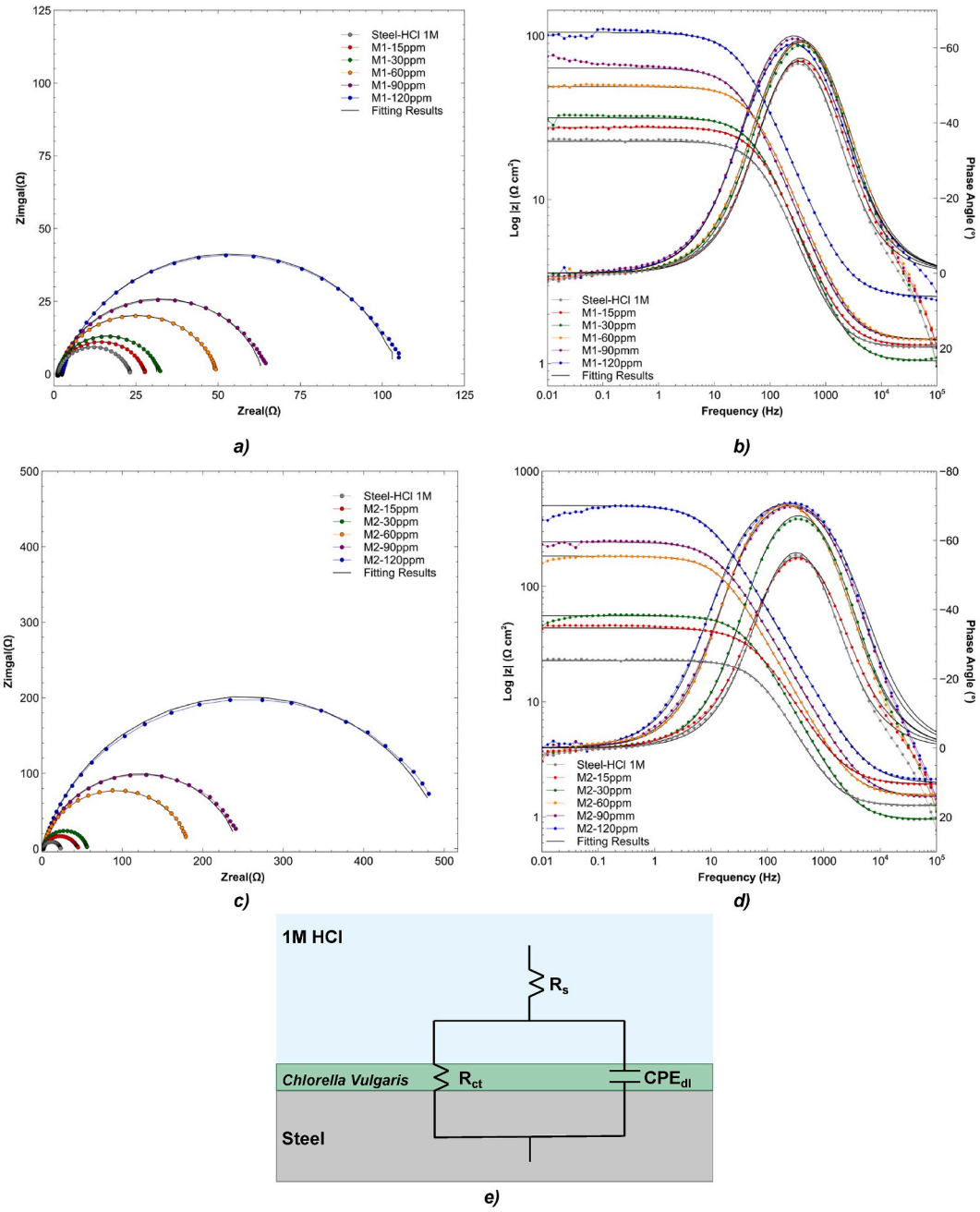

Fig. 4. Electrochemical measurements: (a) Nyquist plot and b) Bode plots of Log |z| and phase angle for M1 extract, c) Nyquist plot and d) Bode plots of Log |z| and phase angle for M2 extract, and e) Equivalent circuit for fitting.

These findings are consistent with previous studies where microalgae such as *Spirulina maxima* [47] and *Chlorella sorokiniana* [84] achieved inhibition efficiencies of 96.4 % and 94.6 %, respectively. *Arthrospira platensis* showed 66 % efficacy [50], *Scenedesmus* sp. achieved up to 95.1 % inhibition [51], and *Chlorococcum* sp. demonstrated a 96 % inhibition rate [52], further supporting the high effectiveness of microalgae as green corrosion inhibitors for steel in acidic environments.

A one-way ANOVA was conducted to determine the influence of biomass concentration in the extract on the corrosion rate mitigated by the inhibitor. The results indicate that with 95 % confidence, the microalgae concentration significantly influences the steel corrosion rate using M1 and M2 as inhibitors (p-value M1: 2.5915E-13 and p-value M2: 5.7691E-15).

Table 2
Fitting results of EIS for M1 and M2 extract.

Sample		R_s (Ω-cm^2)	R_{ct} (Ω-cm^2)	Q (Ω^{-1} sn cm^{-1})	C_{dl} (F cm^{-2})	n	η(%)
Steel - 1M HCL		1,25	21,47	178.6	403.94	0,91	
M1	**15 ppm**	1,29	26,24	22.11	44.84	0,90	18.20
	30 ppm	1,31	33,77	18.13	40.07	0,89	36.42
	60 ppm	1,33	49,97	17.45	40.29	0,89	57.03
	90 ppm	1,37	63,45	11.64	37.34	0,85	66.16
	120 ppm	2,52	102,30	10.23	31.73	0,86	79.01
M2	**15 ppm**	1,92	42,60	14.96	46.75	0,85	49.60
	30 ppm	1,63	55,58	13.14	27.34	0,90	61.37
	60 ppm	1,54	182,20	9.07	22.67	0.89	88.22
	90 ppm	1,67	245,74	8.74	22.58	0.83	91.26
	120 ppm	1,64	501,80	6.25	22.07	0,85	95.72

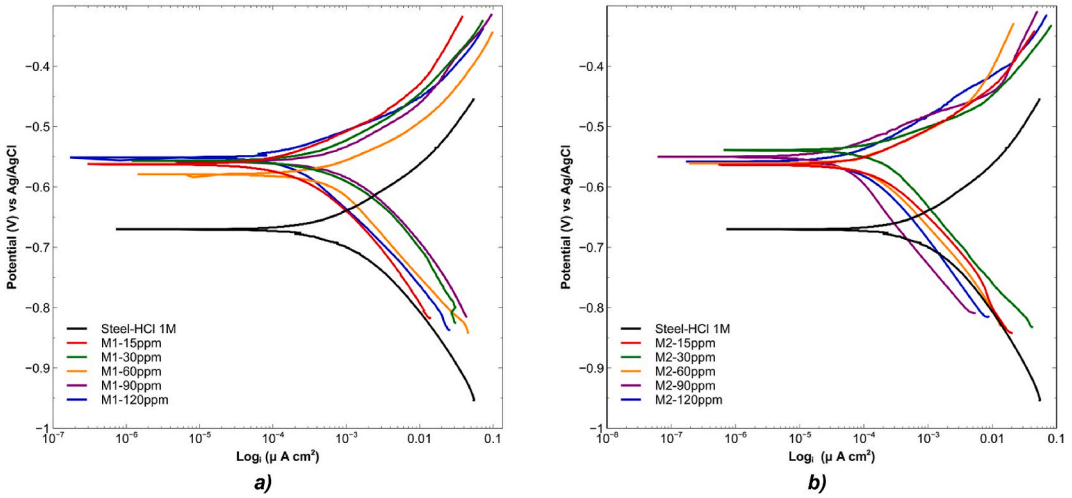

Fig. 5. Polarization curves for a) M1 and b) M2 extracts.

Table 3
Fitting result of polarization curves for M1 and M2 extracts.

Sample		β_a (mV/decade)	β_c (mV/decade)	I_{corr} (μA/cm^2)	E_{corr} (mV-Ag/AgCl)	%η
Steel – 1M HCL		92.3	96,5	622,0	−670,0	–
M1	**15 ppm**	80.9	92.3	140.0	−564.0	77.49 %
	30 ppm	48.7	110.9	157.0	−539.0	74.76 %
	60 ppm	61.9	114.2	122.0	−561.0	80.39 %
	90 ppm	62.2	147.9	53.2	−550.0	91.45 %
	120 ppm	34.2	46.1	17.8	−558.0	97.14 %
M2	**15 ppm**	65.3	85.4	141.0	−562.0	77.33 %
	30 ppm	67.6	85.3	206.0	−616.0	66.88 %
	60 ppm	29.7	56.9	136.0	−579.0	78.14 %
	90 ppm	24.8	26.4	35.9	−560.0	94.23 %
	120 ppm	16.5	29.8	5.7	−551.0	99.09 %

3.5. Adsorption isotherm

To evaluate the interaction of *Chlorella vulgaris* biomass constituents with the metallic surface, adsorption isotherms were used, including Langmuir (Fig. 8a and b), Temkin (Fig. 8c and d), and Frumkin (Fig. 8e and f), models for M1 and M2 respectively. These isotherms relate the degree of surface coverage (θ) to the inhibitor concentration, as described by Equations (8)–(10).

$$\text{Lagmuir Isotherm}\,\frac{\theta}{(1-\theta)} = kC \tag{8}$$

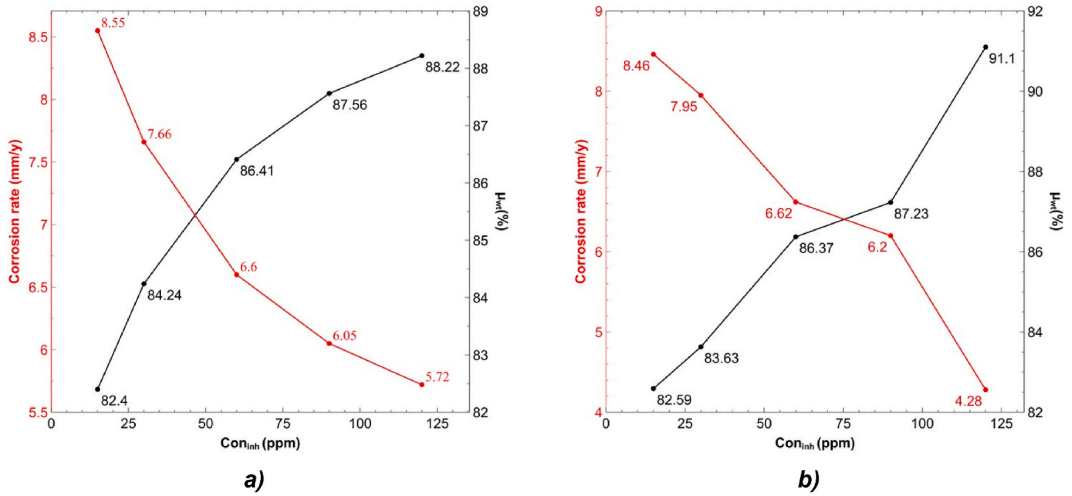

Fig. 6. Corrosion rate and inhibition efficiencies of a) M1 and b) M2.

$$\text{Temkin Isotherm} \log\frac{\theta}{C} = \log K - g\theta \tag{9}$$

$$\text{Frumkin Isotherm} \log\frac{\theta}{(1\text{-}\theta)C} = \log K + g\theta \tag{10}$$

Where C represents the inhibitor concentration in mol/L, K is the equilibrium constant of the inhibitor adsorption process, θ is the coverage factor obtained from Equation (4), and g is the adsorbate interaction parameter [84,88].

Fig. 7 illustrates the linear fit of the adsorption isotherms described by Equations (8)–(10). It is evident that the Langmuir isotherm provides the best linear correlation, with R^2 values of 0.991 and 0.9929 for M1 and M2, respectively.

The Langmuir model assumes that the inhibitor forms a monolayer on the metallic surface, with each active site occupied by inhibitor molecules present in M1 and M2 (Fig. 8). This observation is supported by various studies, indicating a strong interaction between the adsorbed inhibitor molecules and the metallic surface [84,88].

The Gibbs free energy value ΔG^0_{ad} was calculated from Langmuir isotherm using equation (11).

$$\Delta G^0_{ad} = -RT\ln(K_{ads}) \tag{11}$$

Where R is the ideal gas constant (8.314 × 10-3 kJmol-1. K-1) and T is the absolute temperature in Kelvin, and *Kads* value corresponding to the inverse of the slope of the applied fit.

The Gibbs free energy was determined to be −16.88 kJ mol−1 for M1 and -17.11 kJ mol−1 for M2. An absolute ΔG^0_{ad} value of less than 20 kJ mol−1 suggests that M1 and M2 adsorbs onto the carbon steel via a physisorption mechanism [89]. The negative value indicates that the adsorption of M1 and M2 on the carbon steel surface is spontaneous. This implies that the electronic structure perturbation of the adsorbate occurred due to electrostatic interaction with the carbon steel surface [90]. These findings are consistent with the results obtained from electrochemical and gravimetric techniques.

3.6. UV–visible spectroscopy

Fig. 9 displays the UV–Vis spectra of M1 and M2 before and after the immersion of carbon steel for 3 h. Both M1 and M2 exhibited absorption bands at 230 nm corresponding to $\pi \rightarrow \pi^*$ transitions prior to immersion. M1 also showed an additional band at 285 nm, while M2 displayed a band at 271 nm, indicative of intramolecular transfers.

Post-immersion, notable changes were observed in the absorption spectra of the inhibitors. M1 exhibited a shift to higher wavelengths and a new absorbance peak at 332 nm (Fig. 9a). Conversely, M2 demonstrated an increase in absorbance and band intensity at 271 nm, along with a new peak at 340 nm (Fig. 9b). These changes suggest the formation of complexes between Fe^{2+} and the inhibitors, M1 and M2, in 1 M HCl. This is supported by studies indicating that increased absorbance reflects complex formation in solution, providing strong evidence for the potential interaction between the inhibitors and the metal surface [83].

3.7. Surface analysis

The surface morphology of the steel was analyzed based on the protection generated at each evaluated concentration. Fig. 10a and 10b depicts the steel surface before and after exposure to 1M HCl, respectively. Fig. 10a, e, g, i and k illustrate the steel surface after

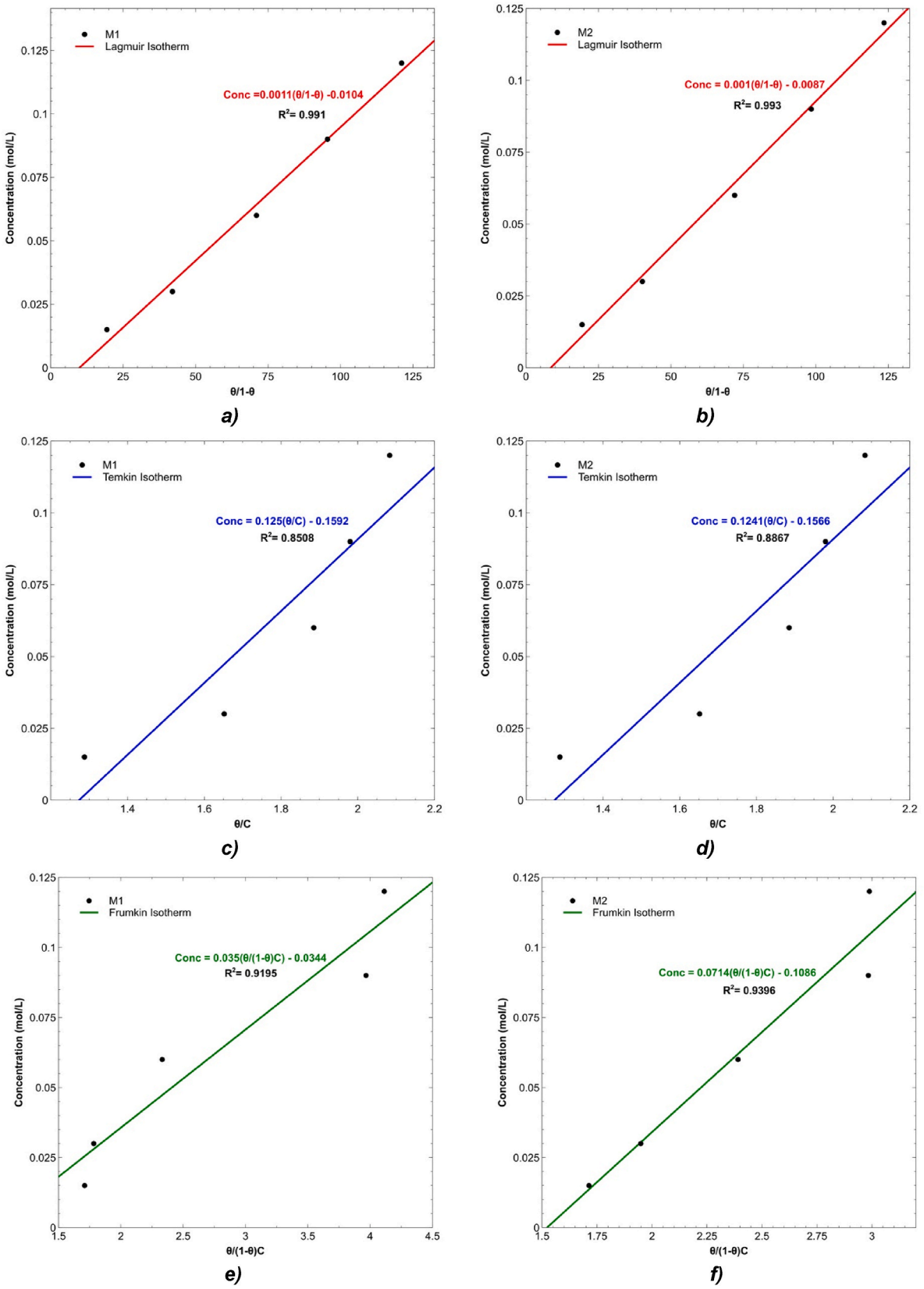

Fig. 7. Adsorption Isotherms for M1 and M2: a) and b) Langmuir, c) and d) Temkin, e) and f) Frumkin Isotherms.

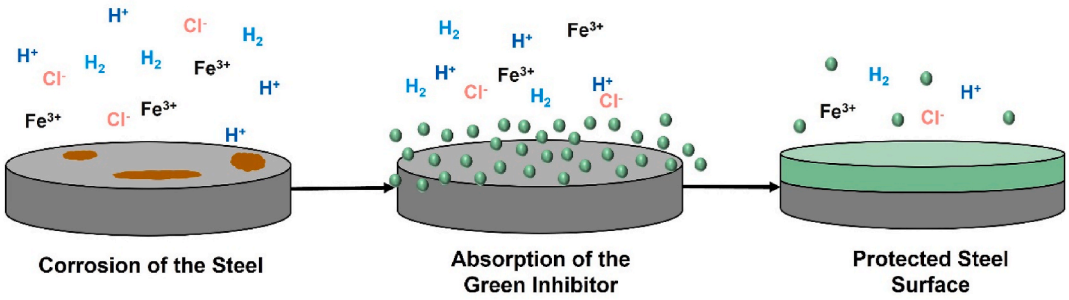

Fig. 8. Absorption mechanism of the green inhibitor.

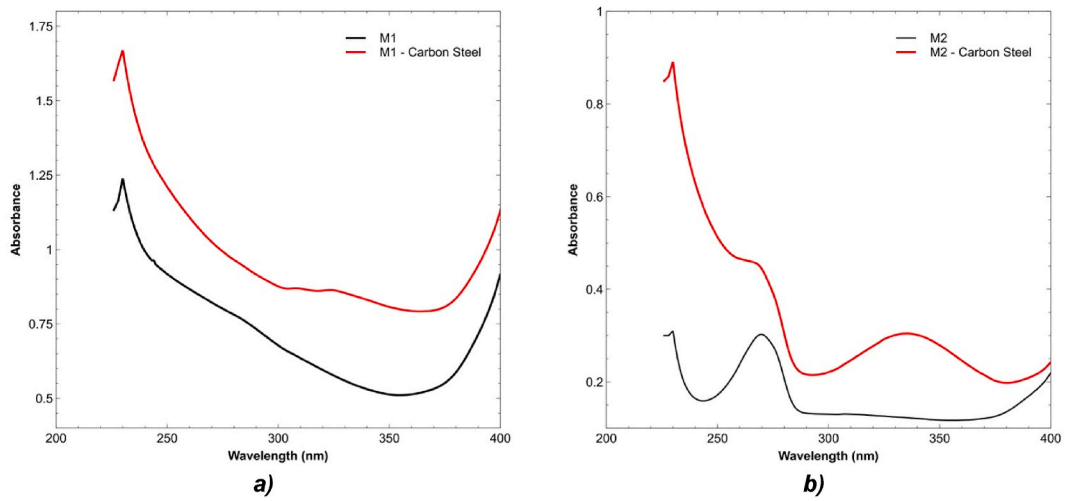

Fig. 9. UV–Vis Spectra of M1 and M2 Before and After Carbon Steel Immersion: a) M1, b) M2.

immersion in 1M HCl with inhibitors M1 and Fig. 10d, f, h, j,and l M2 at each concentration evaluated. The aggressive attack caused by immersion in 1M HCl on API X42 steel is evident on Fig. 10b, even showing superficial loss of material.

Once the inhibitor is added to the immersion solution, and as the concentration of the inhibitors increases, a more homogeneous surface with reduced roughness or less impact from pitting and material loss is observed. This further corroborates the barrier effect generated by inhibitors M1 and M2 against corrosion reactions in acidic media, with the best performance observed at concentrations around 120 ppm.

4. Conclusions, future research and limitations

Chlorella vulgaris extracts (M1 and M2) demonstrated strong corrosion protection, with increasing concentrations leading to enhanced resistance. The highest performance was observed at a concentration of 120 ppm for both inhibitors, with M2 offering superior protection. M2 achieved a charge transfer resistance (R_{ct}) of 501.80 Ω and an inhibition efficiency of 91.20 %, making it the most effective among the tested concentrations. Surface analysis using scanning electron microscopy confirmed the protective effect on the steel surface after exposure to 1M HCl, with M2 at 120 ppm showing the best surface condition, indicating optimal performance against corrosion. Additionally, UV–Vis absorbance results suggested the formation of complexes between Fe^{2+} and the inhibitors, further supporting the inhibitory action of the extracts.

The corrosion inhibition efficiencies of *Chlorella vulgaris* extracts are notably higher at lower concentrations compared to other reported microalgal species. In acidic environments, M1 and M2 achieved inhibition efficiencies of 79.01 % and 95.72 %, respectively. The adsorption of M1 and M2 was well-described by the Langmuir isotherm, with negative ΔG° values confirming the spontaneous and physical nature of the adsorption process. Electrochemical impedance spectroscopy (EIS) results showed a direct correlation between increased concentration and higher charge transfer resistance. The use of a methanol/chloroform solvent mixture in the extraction process significantly enhanced the protective effect of the extracts on the carbon steel surface.

In summary, inhibitors derived from *Chlorella vulgaris* biomass show great potential for acidification processes. Future research should aim to improve the extraction methods to further enhance the performance of M1 and M2, as well as investigate the long-term stability of these inhibitors in acidic environments. This study provides a detailed understanding of the preparation and the interfacial

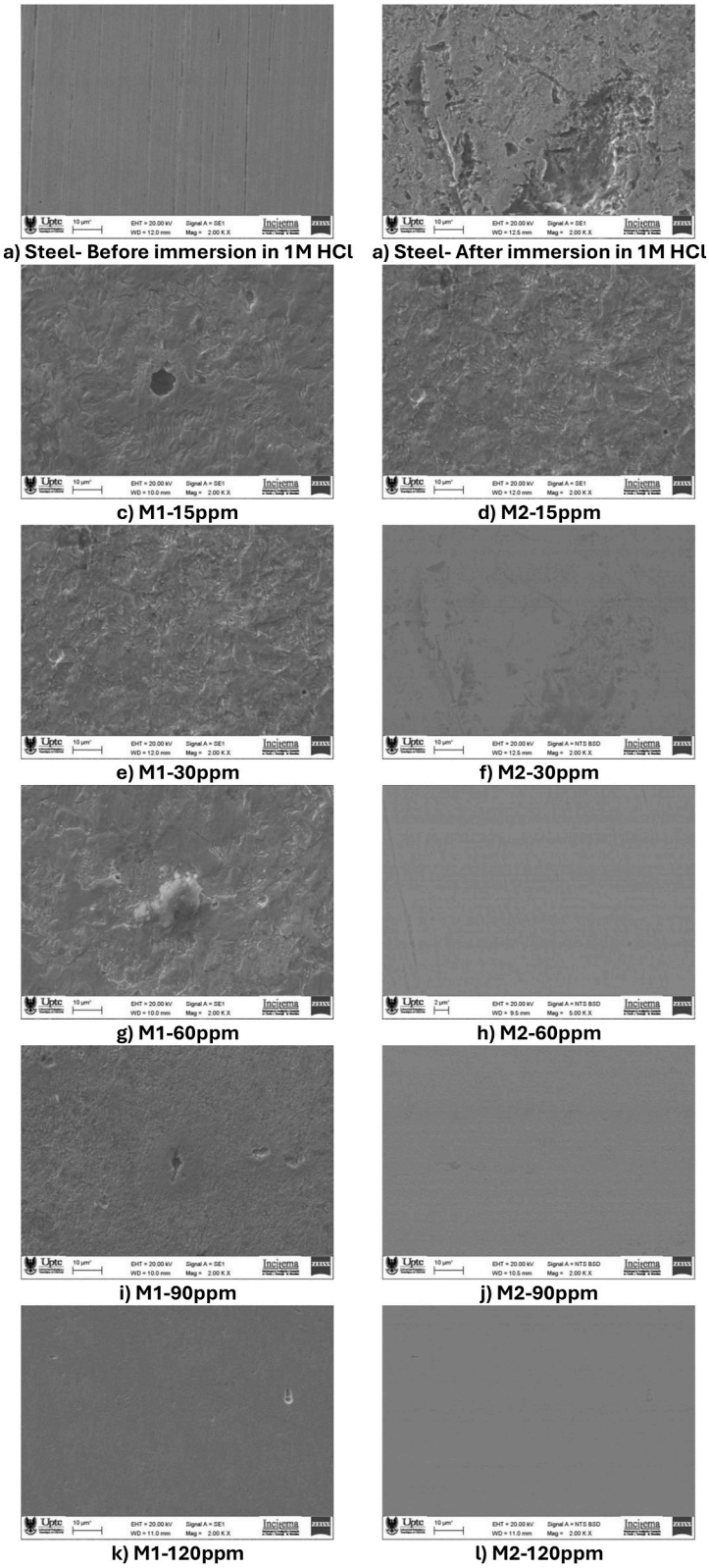

Fig. 10. Surface morphology by SEM at 2000× of: a) Steel – before immersion in 1M HCl, b) Steel – after immersion in 1M HCl, c) M1-15PPM, d) M2-15PPM, e) M1-30PPM, f) M2-30PPM, g) M1-60PPM, h) M2-60PPM, i) M1-90PPM, j) M2-90PPM, k) M1-120PPM, and l) M2-120PPM.

corrosion inhibition mechanisms of these eco-friendly inhibitors.

Based on the findings of this study, several key areas for future research are identified. First, the long-term stability of the microalgae-based inhibitors needs to be investigated, as the current study primarily focused on short-term immersion tests. Evaluating their durability and effectiveness under real-world conditions, including fluctuating temperatures and pH levels, is crucial for understanding their practical application. Additionally, while the laboratory-scale results are promising, scaling up the use of microalgae extracts for industrial applications presents challenges. Factors such as consistency in extract composition, cost-effectiveness of large-scale production, and the impact of environmental conditions on microalgae growth need to be addressed. Furthermore, exploring the potential degradation of the organic compounds in the extracts over time, particularly under prolonged exposure to acidic environments, is important, as this could affect the long-term performance of the inhibitors.

This study also acknowledges that some additional tests, such as X-ray Photoelectron Spectroscopy (XPS), could provide further insights into the surface interactions of the inhibitors. Additionally, the variability in the composition of microalgae extracts, influenced by factors such as cultivation conditions (e.g., light, nutrients, temperature), was not examined. This variability may affect the consistency of inhibitor performance. Standardizing the production process of the extracts could address this issue in future research.

CRediT authorship contribution statement

Edgar Almanza: Writing – original draft, Validation, Methodology, Investigation, Conceptualization. **Lizeth Del Carmen Gutierrez Pua:** Writing – review & editing, Visualization, Validation, Methodology, Formal analysis, Conceptualization. **Yaneth Pineda:** Writing – review & editing, Resources, Investigation, Conceptualization. **Wilson Rozo:** Writing – review & editing, Resources, Investigation, Conceptualization. **Mauricio Marquez:** Writing – review & editing, Supervision, Investigation, Formal analysis, Conceptualization. **Ana Fonseca:** Writing – review & editing, Supervision, Resources, Investigation, Formal analysis, Conceptualization.

Data availability

Any additional information required to reanalyze the data reported in this paper is available from the lead contact upon request. This paper does not report original code.

Lead contact

Further information and requests for resources and reagents should be directed to and will be fulfilled by the lead contact, Ana Fonseca Reyes (fonsecama@uninorte.edu.co).

Funding sources

This research did not receive any specific grant from funding agencies in the public, commercial, or not-for-profit sectors.

Declaration of competing interest

The authors declare that they have no known competing financial interests or personal relationships that could have appeared to influence the work reported in this paper.

Acknowledgements

The authors acknowledge the support given by the Biotechnology laboratory of Universidad del Norte.

References

[1] G. Fu, W. Yang, C.Q. Li, W. Shi, Reliability analysis of corrosion affected underground steel pipes considering multiple failure modes and their stochastic correlations, Tunn. Undergr. Space Technol. 87 (2019) 56–63.
[2] M. Ahammed, R.E. Melchers, Probabilistic analysis of underground pipelines subject to combined stresses and corrosion, Eng. Struct. 19 (12) (1997) 988–994.
[3] C. Lam, W. Zhou, Statistical analyses of incidents on onshore gas transmission pipelines based on PHMSA database, Int. J. Pres. Ves. Pip. 145 (2016) 29–40.
[4] A. Liu, K. Chen, X. Huang, J. Chen, J. Zhou, W. Xu, Corrosion failure probability analysis of buried gas pipelines based on subset simulation, J. Loss Prev. Process. Ind. 57 (2019) 25–33.
[5] A. Agala, M. Khan, A. Starr, Degradation mechanisms associated with metal pipes and the effective impact of LDMs and LLMs in water transport and distribution, Proc. Inst. Mech. Eng. Part C J. Mech. Eng. Sci. 237 (8) (2023) 1855–1876.
[6] Tsyrul nyk, N. V Kret, V.A. Voloshyn, O.I. Zvirko, A procedure of laboratory degradation of structural steels, Mater. Sci. 53 (5) (2018) 674–683.
[7] H. Nykyforchyn, H. Krechkovska, O. Student, O. Zvirko, Feature of stress corrosion cracking of degraded gas pipeline steels, Procedia Struct. Integr. 16 (2019) 153–160.
[8] G. Koch, Cost of corrosion, Trends Oil Gas Corros. Res. Technol. Prod. Transm. (2017) 3–30.
[9] C.I. Ossai, Advances in asset management techniques: an overview of corrosion mechanisms and mitigation strategies for oil and gas pipelines, Int. Sch. Res. Notices 2012 (1) (2012) 570143.
[10] C. Powers, Pipeline Corrosion Protection Methods, Buckaroos, 2024.
[11] Z. Shang, J. Zhu, Overview on plant extracts as green corrosion inhibitors in the oil and gas fields, J. Mater. Res. Technol. 15 (2021) 5078–5094.

[12] M.J. Palimi, et al., Improve the tribo-corrosion behavior of oil-in-water emulsion-based drilling fluids by new derivatives of fatty acid-based green inhibitors, Tribol. Int. 174 (2022) 107723.
[13] M.A. Quraishi, D.S. Chauhan, V.S. Saji, Heterocyclic biomolecules as green corrosion inhibitors, J. Mol. Liq. 341 (Nov. 2021) 117265.
[14] X.L. Fan, C.Y. Li, Y.B. Wang, Y.F. Huo, S.Q. Li, R.C. Zeng, Corrosion resistance of an amino acid-bioinspired calcium phosphate coating on magnesium alloy AZ31, J. Mater. Sci. Technol. 49 (2020) 224–235.
[15] D.S. Chauhan, M.A. Quraishi, V. Srivastava, J. Haque, B. El ibrahimi, Virgin and chemically functionalized amino acids as green corrosion inhibitors: influence of molecular structure through experimental and in silico studies, J. Mol. Struct. 1226 (2021) 129259.
[16] S.O. Ajeigbe, M. Aziz, N. Basar, Adsorption and thermodynamic characteristics of phenylpropanoids of alpinia galanga as corrosion inhibitors on mild steel, Adv. Sci. Lett. 24 (5) (2018) 3561–3567.
[17] M.A. Deyab, E. Guibal, Enhancement of corrosion resistance of the cooling systems in desalination plants by green inhibitor, Sci. Rep. 10 (1) (2020) 1–13, 2020.
[18] G. Ji, S.K. Shukla, P. Dwivedi, S. Sundaram, R. Prakash, Inhibitive effect of argemone mexicana plant extract on acid corrosion of mild steel, Ind. Eng. Chem. Res. 50 (21) (2011) 11954–11959.
[19] S. Deng, X. Li, Inhibition by Ginkgo leaves extract of the corrosion of steel in HCl and H2SO4 solutions, Corrosion Sci. 55 (2012) 407–415.
[20] N. Hossain, M.A. Chowdhury, M. Rana, M. Hassan, S. Islam, Terminalia arjuna leaves extract as green corrosion inhibitor for mild steel in HCl solution, Results Eng 14 (2022) 100438.
[21] M. Srivastava, P. Tiwari, S.K. Srivastava, A. Kumar, G. Ji, R. Prakash, Low cost aqueous extract of Pisum sativum peels for inhibition of mild steel corrosion, J. Mol. Liq. 254 (2018) 357–368.
[22] P.B. Raja, M.G. Sethuraman, Solanum nigrum as natural source of corrosion inhibitor for mild steel in sulphuric acid medium, Corrosion Eng. Sci. Technol. 45 (6) (2010) 455–460.
[23] P.B. Raja, M.G. Sethuraman, Studies on the inhibitive effect of datura stramonium extract on the acid corrosion of mild steel, SRL 14 (6) (2007) 1157–1164.
[24] P.B. Raja, M.G. Sethuraman, Studies on the inhibition of mild steel corrosion by Rauvolfia serpentina in acid media, J. Mater. Eng. Perform. 19 (5) (2010) 761–766.
[25] K.O. Orubite, N.C. Oforka, Inhibition of the corrosion of mild steel in hydrochloric acid solutions by the extracts of leaves of Nypa fruticans Wurmb, Mater. Lett. 58 (11) (2004) 1768–1772.
[26] E.E. Oguzie, Studies on the inhibitive effect of Occimum viridis extract on the acid corrosion of mild steel, Mater. Chem. Phys. 99 (2–3) (2006) 441–446.
[27] N. El Hamdani, R. Fdil, M. Tourabi, C. Jama, F. Bentiss, Alkaloids extract of Retama monosperma (L.) Boiss. seeds used as novel eco-friendly inhibitor for carbon steel corrosion in 1 M HCl solution: electrochemical and surface studies, Appl. Surf. Sci. 357 (2015) 1294–1305.
[28] P.M. Krishnegowda, V.T. Venkatesha, P.K.M. Krishnegowda, S.B. Shivayogiraju, Acalypha torta leaf extract as green corrosion inhibitor for mild steel in hydrochloric acid solution, Ind. Eng. Chem. Res. 52 (2) (2013) 722–728.
[29] A.Y. El-Etre, M. Abdallah, Z.E. El-Tantawy, Corrosion inhibition of some metals using lawsonia extract, Corrosion Sci. 47 (2) (2005) 385–395.
[30] M. Abdallah, M.A. Radwan, S.M. Shohayeb, S. Abdelhamed, Use of some natural oils as crude pipeline corrosion inhibitors in sodium hydroxide solutions, Chem. Technol. Fuels Oils 46 (5) (2010) 354–362.
[31] M. Abdallah, H.M. Altass, B.A.A.L. Jahdaly, M.M. Salem, Some natural aqueous extracts of plants as green inhibitor for carbon steel corrosion in 0.5 M sulfuric acid, Green Chem. Lett. Rev. 11 (3) (2018) 189–196.
[32] B.R. Pandian, M.G. Sethuraman, Solanum tuberosum as an inhibitor of mild steel corrosion in acid media, Iran. J. Chem. Chem. Eng. 28 (1) (2009) 77–84.
[33] K. Dob, E. Zouaoui, D. Zouied, Corrosion inhibition of curcuma and saffron on A106 Gr B carbon steel in 3% NaCl medium, Anti-corrosion Methods & Mater. 65 (3) (2018) 225–233.
[34] A.A. Khadom, M.M. Kadhim, R.A. Anaee, H.B. Mahood, M.S. Mahdi, A.W. Salman, Theoritical evaluation of Citrus Aurantium leaf extract as green inhibitor for chemical and biological corrosion of mild steel in acidic solution: statistical, molecular dynamics, docking, and quantum mechanics study, J. Mol. Liq. 343 (2021) 116978.
[35] A. Boutoumit, et al., Electrochemical, structural and thermodynamic investigations of methanolic parsley extract as a green corrosion inhibitor for C37 steel in HCl, Coatings 14 (7) (2024) 783.
[36] E. Alibakhshi, M. Ramezanzadeh, G. Bahlakeh, B. Ramezanzadeh, M. Mahdavian, M. Motamedi, Glycyrrhiza glabra leaves extract as a green corrosion inhibitor for mild steel in 1 M hydrochloric acid solution: experimental, molecular dynamics, Monte Carlo and quantum mechanics study, J. Mol. Liq. 255 (2018) 185–198.
[37] C.M. Fernandes, et al., Ircinia strobilina crude extract as corrosion inhibitor for mild steel in acid medium, Electrochim. Acta 312 (2019) 137–148.
[38] F.E. Abeng, et al., Insight into corrosion inhibition mechanism of carbon steel in 2 M HCl electrolyte by eco-friendly based pharmaceutical drugs, Chem. Data Collect. 34 (Aug. 2021) 100722.
[39] C. Kamal, M.G. Sethuraman, Caulerpin-A bis-indole alkaloid as a green inhibitor for the corrosion of mild steel in 1 M HCl solution from the marine alga caulerpa racemosa, Ind. Eng. Chem. Res. 51 (31) (2012) 10399–10407.
[40] C. Kamal, M.G. Sethuraman, Hydroclathrus clathratus marine alga as a green inhibitor of acid corrosion of mild steel, Res. Chem. Intermed. 39 (8) (2013) 3813–3828.
[41] G.G.P. De Souza, et al., Study of the efficiency of the algae Prasiola crispa extract as a corrosion inhibitor in HCl 1 mol L-1, Rev. Virtual Quim. 11 (5) (2019) 1521–1529.
[42] A. Hernández-Pérez, J.I. Labbé, Microalgae, culture and benefits, Rev. Biol. Mar. Oceanogr. 49 (2) (2014) 157–173.
[43] S. Lage, A. Willfors, A. Hörnberg, F.G. Gentili, Impact of organic solvents on lipid-extracted microalgae residues and wastewater sludge co-digestion, Bioresour. Technol. Rep. 16 (2021) 100850.
[44] S.Y.A. Siddiki, et al., Microalgae biomass as a sustainable source for biofuel, biochemical and biobased value-added products: an integrated biorefinery concept, Fuel 307 (2022) 121782.
[45] E. Couto, M.L. Calijuri, P. Assemany, Biomass production in high rate ponds and hydrothermal liquefaction: wastewater treatment and bioenergy integration, Sci. Total Environ. 724 (2020) 138104.
[46] S.Y.A. Siddiki, et al., Microalgae biomass as a sustainable source for biofuel, biochemical and biobased value-added products: an integrated biorefinery concept, Fuel 307 (September 2021) (2022) 121782.
[47] L.S. Rodrigues, A.F. do Valle, E. D'Elia, Biomass of microalgae Spirulina maxima as a corrosion inhibitor for 1020 carbon steel in acidic solution, Int. J. Electrochem. Sci. 13 (7) (2018) 6169–6189.
[48] G.A. de Oliveira, et al., Biomass of microalgae Chlorella sorokiniana as green corrosion inhibitor for mild steel in HCl solution, Int. J. Electrochem. Sci. 16 (2) (2021) 210249.
[49] C. Kamal, M.G. Sethuraman, Spirulina platensis – a novel green inhibitor for acid corrosion of mild steel, Arab. J. Chem. 5 (2) (2012) 155–161.
[50] B. Anwar, T. Khairunnisa, Y. Sunarya, Corrosion inhibition of a516 carbon steel in 0.5 m hcl solution using arthrospira platensis extract as green inhibitor, Int. J. Corros. Scale Inhib. 9 (1) (2020) 244–256.
[51] A. Khanra, M. Srivastava, M.P. Rai, R. Prakash, Application of unsaturated fatty acid molecules derived from microalgae toward mild steel corrosion inhibition in HCl solution: a novel approach for metal-inhibitor association, ACS Omega 3 (10) (Oct. 2018) 12369–12382.
[52] M. Prakash, A. Khanra, S. Rai, M. Srivastava, R. Prakash, Application of Unsaturated role of levoglucosenone and hexadecanoic acid from microalgae Chlorococcum sp . for corrosion resistance on mild steel : electrochemical , microstructural and theoretical analysis, J. Mol. Liq. 266 (2018) 279–290.
[53] C. Safi, B. Zebib, O. Merah, P.Y. Pontalier, C. Vaca-Garcia, Morphology, composition, production, processing and applications of Chlorella vulgaris: a review, Renew. Sustain. Energy Rev. 35 (2014) 265–278.
[54] N.E.A. El-Naggar, M.H. Hussein, S.A. Shaaban-Dessuuki, S.R. Dalal, Production, extraction and characterization of Chlorella vulgaris soluble polysaccharides and their applications in AgNPs biosynthesis and biostimulation of plant growth, Sci. Rep. 10 (1) (2020) 1–19, 101.
[55] C. Aguoru, P.O. Okibe, Content and composition of lipid produced by chlorella vulgaris for biodiesel production, Adv. Life Sci. Technol. 36 (2015).

[56] Y. Jeong, et al., Marine cyanobacterium Spirulina maxima as an alternate to the animal cell culture medium supplement, Sci. Rep. 11 (1) (2021) 1–11, 111.
[57] R.Y. Kannah, S. Kavitha, O.P. Karthikeyan, E.R. Rene, G. Kumar, J.R. Banu, A review on anaerobic digestion of energy and cost effective microalgae pretreatment for biogas production, Bioresour. Technol. 332 (2021) 125055.
[58] T. Mathimani, E.R. Rene, S. Devanesan, M.S. AlSalhi, R. Shanmuganathan, Assessment of taxonomically diverse Chlorococcum species and Chroococcus species for cell density, pigments, biochemical components, and fatty acid composition for fuel/food applications, Algal Res. 74 (2023) 103228.
[59] N. Gladkikh, et al., Formation of polymer-like anticorrosive films based on organosilanes with benzotriazole, carboxylic and phosphonic acids. Protection of copper and steel against atmospheric corrosion, Prog. Org. Coating 141 (2020) 105544.
[60] Zin, et al., Inhibition of the corrosion of carbon steels by trehalose lipid surfactants, Mater. Sci. 54 (4) (2019) 477–484.
[61] A. Kasprzhitskii, G. Lazorenko, Corrosion inhibition properties of small peptides: DFT and Monte Carlo simulation studies, J. Mol. Liq. 331 (2021) 115782.
[62] N. Chaubey, A. Qurashi, D. Singh Chauhan, M. Quraishi, Frontiers and advances in green and sustainable inhibitors for corrosion applications: Crit. Rev. 321 (1) (2020).
[63] S. Kaya, B. Tüzün, C. Kaya, I.B. Obot, Determination of corrosion inhibition effects of amino acids: quantum chemical and molecular dynamic simulation study, J. Taiwan Inst. Chem. Eng. 58 (2016) 528–535.
[64] M. Ras, J.P. Steyer, O. Bernard, Temperature effect on microalgae: a crucial factor for outdoor production, Rev. Environ. Sci. Biotechnol. 12 (2) (2013) 153–164.
[65] N. Arora, G.P. Philippidis, Insights into the physiology of Chlorella vulgaris cultivated in sweet sorghum bagasse hydrolysate for sustainable algal biomass and lipid production, Sci. Rep. 11 (1) (2021) 1–14, 111.
[66] X. Gu, et al., Engineering a marine microalga Chlorella sp. as the cell factory, Biotechnol. Biofuels Bioprod 16 (1) (2023) 1–9.
[67] M. Al-Hammadi, M. Güngörmüşler, New insights into Chlorella vulgaris applications, Biotechnol. Bioeng. 121 (5) (2024) 1486–1502.
[68] M. Abdallah, H.M. Eltass, M.A. Hegazy, H. Ahmed, Adsorption and inhibition effect of novel cationic surfactant for pipelines carbon steel in acidic solution, Protect. Met. Phys. Chem. Surface 52 (4) (2016) 721–730.
[69] V.A. Grachev, A.E. Rozen, Y.P. Perelygin, S.Y. Kireev, I.S. Los, A.A. Rozen, Measuring corrosion rate and protector effectiveness of advanced multilayer metallic materials by newly developed methods, Heliyon 4 (8) (2018) e00731.
[70] ASTM INTERNATIONAL, s, ASTM G31.Standard Guide for Laboratory Immersion Corrosion Testing of Metal 03.02 (2021).
[71] S.H. Alrefaee, K.Y. Rhee, C. Verma, M.A. Quraishi, E.E. Ebenso, Challenges and advantages of using plant extract as inhibitors in modern corrosion inhibition systems: recent advancements, J. Mol. Liq. 321 (Jan. 2021) 114666.
[72] A.A. Fadhil, A.A. Khadom, S.K. Ahmed, H. Liu, C. Fu, H.B. Mahood, Portulaca grandiflora as new green corrosion inhibitor for mild steel protection in hydrochloric acid: quantitative, electrochemical, surface and spectroscopic investigations, Surface. Interfac. 20 (2020) 100595.
[73] M.T. majd, M. Ramezanzadeh, G. Bahlakeh, B. Ramezanzadeh, Probing molecular adsorption/interactions and anti-corrosion performance of poppy extract in acidic environments, J. Mol. Liq. 304 (2020) 112750.
[74] W. Zeroual, C. Choisy, S.M. Doglia, H. Bobichon, J.F. Angiboust, M. Manfait, Monitoring of bacterial growth and structural analysis as probed by FT-IR spectroscopy, Biochim. Biophys. Acta Mol. Cell Res. 1222 (2) (1994) 171–178.
[75] I. Ponnuswamy, S. Madhavan, S. Shabudeen, Isolation and characterization of green microalgae for carbon sequestration, waste water treatment and bio-fuel production, Int. J. Bio-Science Bio-Technology 5 (2) (2013).
[76] M. Giordano, M. Kansiz, P. Heraud, J. Beardall, B. Wood, D. McNaughton, Fourier transform infrared spectroscopy as a novel tool to investigate changes in intracellular macromolecular pools in the marine microalga chaetoceros muellerii (bacillariophyceae), J. Phycol. 37 (2) (2001) 271–279.
[77] A. Gonzalez-Torres, A.M. Rich, C.E. Marjo, R.K. Henderson, Evaluation of biochemical algal floc properties using Reflectance Fourier-Transform Infrared Imaging, Algal Res. 27 (2017) 345–355.
[78] L. Huang, et al., Exploration of procyanidin C1 from Uncaria laevigata as a green corrosion inhibitor in industry: electrochemical assessment, theoretical simulation, and environmental safety, Sep. Purif. Technol. 318 (December 2022) 123950, 2023.
[79] R. Xu, X. Yang, P. Li, K.W. Suen, G. Wu, P.K. Chu, Eelectrochemical properties and corrosion resistance of carbon-ion-implanted magnesium, Corrosion Sci. 82 (2014) 173–179.
[80] J.N. Murray, Electrochemical test methods for evaluating organic coatings on metals: an update. Part I. Introduction and generalities regarding electrochemical testing of organic coatings, Prog. Org. Coating 30 (4) (1997) 225–233.
[81] X. Wei, et al., Improvement on corrosion resistance and biocompability of ZK60 magnesium alloy by carboxyl ion implantation, Corrosion Sci. 173 (2020) 108729.
[82] F.Z. Eddahhaoui, et al., Experimental and computational aspects of green corrosion inhibition for low carbon steel in HCl environment using extract of Chamaerops humilis fruit waste, J. Alloys Compd. 977 (2024) 173307.
[83] A. Singh, K.R. Ansari, D.S. Chauhan, M.A. Quraishi, H. Lgaz, I.M. Chung, Comprehensive investigation of steel corrosion inhibition at macro/micro level by ecofriendly green corrosion inhibitor in 15% HCl medium, J. Colloid Interface Sci. 560 (2020) 225–236.
[84] G.A. de Oliveira, et al., Biomass of microalgae Chlorella sorokiniana as green corrosion inhibitor for mild steel in HCl solution, Int. J. Electrochem. Sci. 16 (2) (Feb. 2021) 1–22.
[85] Z. Li, J. Song, J. Chen, Q. Yu, K. Xiao, Corrosion behavior of a high-strength steel E690 in aqueous electrolytes with different chloride concentrations, J. Mater. Res. Technol. 22 (2023) 596–604.
[86] S. Chen, et al., Effect of marine microalgae Synechococcus sp., Chlorella sp., Thalassiosira sp. on corrosion behavior of Q235 carbon steel in f/2 medium, Bioelectrochemistry 150 (Apr. 2023) 108349.
[87] J. Hu, W. Liu, Chitosan/tannic acid phenamine networks-hollow mesoporous silica capsules with reversible pH response: controlled-releasing amino acid derivatives as 'green' corrosion inhibitor, Carbohydr. Polym. 320 (July) (2023) 121244.
[88] A. Kokalj, On the use of the Langmuir and other adsorption isotherms in corrosion inhibition, Corrosion Sci. 217 (2023) 111112.
[89] L.T. Popoola, A.S. Yusuff, O.M. Ikumapayi, O.M. Chima, A.T. Ogunyemi, B.A. Obende, Carbon steel behavior towards Cucumeropsis mannii shell extract as an ecofriendly green corrosion inhibitor in chloride medium, Sci. African 21 (2023) e01860.
[90] M.F. Chen, Y. Chen, Z.J. Lim, M.W. Wong, Adsorption of imidazolium-based ionic liquids on the Fe(1 0 0) surface for corrosion inhibition: physisorption or chemisorption? J. Mol. Liq. 367 (2022) 120489.